Predicting Vibrational Mean Free Paths in Amorphous Materials

Jason M. Larkin[1] and A. J. H. McGaughey[2,*]

[1]*Department of Mechanical Engineering*
Carnegie Mellon University
Pittsburgh, PA 15213
[2]*Department of Mechanical Engineering*
Carnegie Mellon University
Pittsburgh, PA 15213

(Dated: June 2, 2013)

Understanding thermal transport in crystalline systems requires detailed knowledge of phonons, which are the quanta of energy associated with atomic vibrations. By definition, phonons are non-localized vibrations that transport energy over distances much larger than the atomic spacing. For disordered materials (e.g., alloys, amorphous phases), with the exception of very long wavelength modes, the vibrational modes are localized and do not propagate like phonons. The Einstein model assumes that the mean free path of these localized vibrations is the average interatomic distance and that their group velocity is equal to the speed of sound. The Cahill-Pohl model assumes that the mean free path of the localized modes is equal to half of their wavelength. While these approach can be used to estimate the thermal conductivity of disordered systems, they only provide a qualitative description of the vibrations that contribute to the lattice thermal conductivity. Using lattice dynamics calculations and molecular dynamics simulations on model amorphous silicon and silica, we predict and characterize the contributions from phonons and localized vibrations to lattice thermal conductivity. The vibrational mean free paths are predicted for these two amorphous materials and the thermal conductivity accumulation function is compared with recent experimental results.

I. INTRODUCTION

The thermal conductivity of amorphous solids display unique temperature dependance compared to ordered solids.[1] Cahill argued that the lattice vibrations in a disordered crystal are essentially the same as those of an amorhous solid.[2]

Measurements by all the refs from Galli paper, including Moon.[3–9] The key to understanding such measurement is to estimate a MFP for the vibrational modes in disordered systems.

The goal of this work is to predict the MFP of vibrational modes in disordered systems. Simple Lennard-Jones systems will be studied. A perfect LJ crystal are alloyed with a species of differing mass and amorphous samples are prepared. Thermal transport will be studied to quantify and characterize the ordered and disordered contributions to lattice thermal conductivity. In particular, a more rigorous way to classify vibrational modes in disordered alloys and amorphous samples as phonon-like or diffuson will be investigated. These results will be compared to the phenomenological Einstein and Cahill-Pohl models,[? ? ?] .

The vibrational modes in these systems are characterized in the limit of propagating (phonon) and non-propagating (diffuson) modes by predicting the mode lifetimes and estimating their mean free paths. Estimating an effective dispersion relation is necessary for calculating an effective group velocity for disordered, which is crucial for transforming lifetimes to MFPs. The spectrum of phonon MFPs and the accumulated thermal conductivity are predicted for a model of amorphous silicon. Predictions of thermal conductivity using a boundary scattering model demonstrates

II. THEORETICAL FORMULATION

A. Phonons

For a perfect lattice, all vibrational modes are phonon modes, which by definition are delocalized, propagating plane waves.[10] In an amorphous system, only in the low-frequency, long-wavelength limit can the vibrational modes be considered phonons. Identifying this limit is crucial to quantify the contribution of phonon-like modes in a-Si and a-SiO_2 (see Section).

Using the single-mode relaxation time approximation[10] to solve the Boltzmann transport equation gives an expression for thermal conductivity,

$$k_{ph} = \sum_{\boldsymbol{\kappa}} \sum_{\nu} c_{ph}(\boldsymbol{\kappa}_\nu)\, \boldsymbol{v}_g^2(\boldsymbol{\kappa}_\nu)\, \tau(\boldsymbol{\kappa}_\nu)\,. \tag{1}$$

In general, the thermal conductivity k_{ph} and group velocity $\boldsymbol{v}_g(\boldsymbol{\kappa}_\nu)$ depend on the spatial direction $\mathbf{n}$. Since the amorphous materials studied in this work are isotropic, k_{ph} and v_g are quantities indepdent of the direction $\mathbf{n}$.

For Eq. , the sum is over the phonon modes in the first Brillouin zone, $\boldsymbol{\kappa}$ is the wave vector, and ν labels the polarization branch. The phonon mode has frequency $\omega(\boldsymbol{\kappa}_\nu)$, volumetric specific heat $C_{ph}(\boldsymbol{\kappa}_\nu)$, group velocity vector $\boldsymbol{v}_{g,\mathbf{n}}(\boldsymbol{\kappa}_\nu)$, and lifetime $\tau(\boldsymbol{\kappa}_\nu)$. The phonon mean free path

(MFP),

$$\Lambda(\boldsymbol{\kappa}_\nu) = |\boldsymbol{v}_g^2(\boldsymbol{\kappa}_\nu)|\tau(\boldsymbol{\kappa}_\nu), \tag{2}$$

is the distance the phonon travels before scattering. The transformation from lifetime to MFP requires a group velocity.

Because there is a spectrum of vibrational modes in cyrstalline and amorphous systems, there are typically a range of vibrational MFPs.(cite) By reducing the system feature sizes, the vibrational MFPs can be reduced due to boundary scattering.(cite)

Taking the phonon mode specific heat to be $c_{ph}(\boldsymbol{\kappa}_\nu) = k_B$, the phonon mode specific vibrational conductivity (Eq. (**??**)) can be written as

$$k_{ph,\mathbf{n}} = \sum_{\boldsymbol{\kappa}} \sum_{\nu} k_B D_{ph}(\boldsymbol{\kappa}_\nu), \tag{3}$$

and the vibrational conductivity is determined by the phonon mode diffusitivies, defined as

$$D_{ph}(\boldsymbol{\kappa}_\nu) = v(\boldsymbol{\kappa}_\nu)^2 \tau(\boldsymbol{\kappa}_\nu). \tag{4}$$

B. Diffusons

For disordered systems, the vibrational modes are no longer pure plane-waves (i.e., phonon modes), except in the low-frequency (long-wavelength) limit. When applied in the classical limit, the Allen-Feldman (AF) theory computes the contribution of diffusive, non-propagating modes (i.e., diffusons) to thermal conductivity[11]

$$k_{AF} = \sum_{diffusons} \frac{k_\mathrm{B}}{V} D_{AF,i}(\omega_i), \tag{5}$$

where $D_{AF,i}$ is the mode diffusivity and ω_i is the frequency of the ith diffuson. The diffusivity of diffusons can be calculated from harmonic lattice dynamics theory.[11–13]

The relative contribution of both phonons and diffusons to the total vibrational conductivity has been estimated to be approximately equal for a model of a-Si,[14] while earlier studies find that k_{ph} is somewhat less.[12,13]

C. Thermal Diffusivity Limits

k = sum c D, only for low-w, long-lambda limit does D = 1/3 $v^2 tau, or 1/3 v Lambda$

"The diffusivity D i cannot be meaningfully represented as v 2 i /3 since v i and i cannot be independently i defined. Numerically we find that D i for diffusons is of order D a/3 where a is the interparticle spacing. Also, D i is inde- pendent of the particular state i, depending only on the en- ergy as seen in Fig. 12. Our Eq. 7 for the heat conductivity is a close analog of Eq. A4.

$$\tau = \frac{2\pi}{\omega}. \tag{6}$$

$$\Lambda = \lambda. \tag{7}$$

It is not clear that these limits are equivalent if the group velocity is mode-dependent.

A high-scatter limit for the mode diffusivity is

$$D_{HS} = \frac{1}{3} v_s a, \tag{8}$$

where it is assumed that all vibrational modes travel with the sound speed, v_s, and scatter over a distance of the lattice constant, a. This diffusivity assumption leads to a high-scatter (HS) limit of thermal conductivity in the classical limit[15]

$$k_{HS} = \frac{k_\mathrm{B}}{V_b} b v_s a, \tag{9}$$

where V_b is the volume of the unit cell and b is the number of atoms in the unit cell.

It was demonstrated by Birch and Clark and then Kittel that the thermal conductivity of glasses above 20K could be interpreted using a temperature-independent diffusivity on the order of Eq. In the phonon model, this would correspond to a MFP $\Lambda = a$, too small to justify use of the model. The success of this observation implies that the dominant normal modes in most glasses are diffusons and not phonons.

While Eq and are commonly used to establish a high-scatter limit for diffusivity and thermal conductivity, predictions for a-SiGe alloys demonstrated that these are not true high-scatter limits.[12] Recently, the thermal conductivity of several materials has been measured to be significantly below the high-scatter limite Eq. .(cite)

III. CALCULATION DETAILS

A. Sample Preparation

1. *Amorphous Si*

We use models created by the Wooten-Winer-Weaire (WWW) algorithm in Ref. **?** . Sample sizes of 216, 1000, 4096, and 100,000 atoms. The Stillinger-Weber potential is then used with these samples and the denisty ρ is set to kg/m^3, which is equivalent to a crystalline density with a lattice constant of 5.43 $\mathring{A}$.(cite) The samples were annealed at a temperature of 1100 K for 5 ns to remove meta-stability. The meta-stability is demonstrated by increased vs after annealing. structural relaxation: Ul =7.64X10 m/s and UT=3. 67X10, indicates that there has been structural relaxation $vs_long : 8.2715e+03, vs_tran : 3.8867e+03$

With amorphous materials, have to deal with meta-stability.(cite) There are many potential energy configurations (atomic positions) which are nearly equivalent in energy. At a sufficient temperature, the meta-stable states cause the equillibrium atomic positions to vary. This can effect on the prediction of the vibrational mode lifetimes when using the normal mode decomposition method. In the time domain, the average normal mode potential and kinetic energy must be calculated and subtracted from the normal mode energy autocorrelation function. If the average energy is not specified correctly, unphysically large or small mode lifetimes can be predicted.

A large sample (800,000 atoms) was created from the 100,000 atom sample by treating it as a unit cell and tiling the 800,000 atom supercell. The box size is nm.

All calculations based on density of the perfect crystal with lattice constant 5.43 Ang.

Similar structures and results can be obtained with a-Si samples created using a melt-quench-anneal procedure similar to that used to create a-SiO_2 samples in Section . The entire procedure is performed at constnat volume. Crystalline silicon (c-Si) is first melted at a temperature of 10,000 K. The liquid is then quenched instantaneously to 300 K, and then annealed at 1100 K for 10 ns to remove meta-stability.

2. *Amorphous SiO_2*

samples from Alan. The 24-6 LJ potential is replaced with a 12-6, which has a negligible effect on the predictions presented in this paper.

New samples of size up to 4400 atoms were created by first tiling the smaller samples, and then performing a liquid quench procedure similar to Alan. Results for these quenched, fully amorphous samples agree closely with those of the unquenched, tiled samples.

B. Simulation Details

The MD simulations were performed using LAMMPS.[16]

dt = 0.00905 , dt = 0.0005

$2^20 for 10 seeds. For the GK method, the thermal conductivity is predicted by windowed cumulative integral of the heat current autoco$
SiO_2 and s-Si, a interval of the the HCACF integral can be found which is constant within the statistical noise.

The trajectories from the MD simulatoins used for the GK calcaultions (Setion) are also used in the normal mode decomposition method (Section).

The AF calculation is performed using the package GULP. A Lorentzian broadening is used of $5\delta\omega_{avg}$ and $14\delta\omega_{avg}$ for a-Si and a-SiO^2. Varying the broadening around these values does not change the resulting thermal conductivity significantly (see Section).

IV. VIBRATIONAL PROPERTIES

A. Density of States

In this section, we compute the frequencies and density of states (DOS) for the vibrational modes for the models of a-SiO_2 and a-Si described in Section . The frequencies are computed using harmonic lattice dynamics calculations with GULP.[?] For amorphous supercells, the only allowed wave vector is the gamma-point (i.e., $\boldsymbol{\kappa} = 0$), where there are $3N_a$ polarization branches. Calculation of the Gamma modes require the eigenvalue solution of a dynamical matrix of size $(3N_a)^2$ that scales as $[(3N_a)^2]^3$, limiting the system sizes that can be considered. This eigenvalue solution is also required to perform the NMD (see Section **??**) and AF calculations (see Section IV D).

The vibrational DOS is computed by

$$DOS(\omega) = \sum_i \delta\omega_i - \omega, \tag{10}$$

where a unit step function is used to broaden $\delta(\omega_i - \omega)$. The DOS for a-$SiO_2$ and a-Si are plotted in Fig. using two values of broadening, $10\delta\omega_{avg}$ and $100\delta\omega_{avg}$, where $\delta\omega avg$ is the average frequency spacing. Because of the finite model size, the low-frequency modes are sparse and the DOS has a large variability dependent on the broadening.[13] As the system size L is increased, the lowest frequency mode will continue to decrease and the gaps at higher frequency will fill in. However, because of the computational cost of the NMD and AF methods, finite-size (4096 atoms, L = , 4608 atoms, L =) must be used to predict the mode properties and the predicted thermal conductivity compared with that from the Green-Kubo (GK) method (see Section).

While the DOS has a large amount of variability at low frequency, there is a clear scaling of $DOS \propto \omega^{-2}$ for both a-Si and a-SiO_2. The range of this scaling is larger for a-Si than a-SiO_2. Under the Debye model, which assumes isotropic and linear dispersion, the DOS is

$$DOS(\omega) = \frac{3 * \pi\omega^2}{2v_{s,DOS}^3}, \tag{11}$$

where v_s is an appropriate sound speed.(cite) By fitting the DOS from Fig. to Eq. , a sound speed is predicted at reported in Table . For both a-Si and a-SiO_2, the sound speeds predicted from the DOS are close to the transverse sound speeds predicted from the elastic constants and the structure factor. The Debye model predicts that the contribution from the larger longitdunal sound speed compared to the smaller transverse sound speed will scale as the difference cubed. For a-Si, the contribution from longitudinal modes to the Debye DOS is nearly an order of magnitude less than the transverse modes for a given frequency interval. For a-SiO_2, the logitudinal and transverse sound speeds are closer.(cite experimental a-DOS)

This makes sense under the Debye model, which depends inversely on the cube of the sound speed, and predicts a significantly smaller number of logitudinal modes

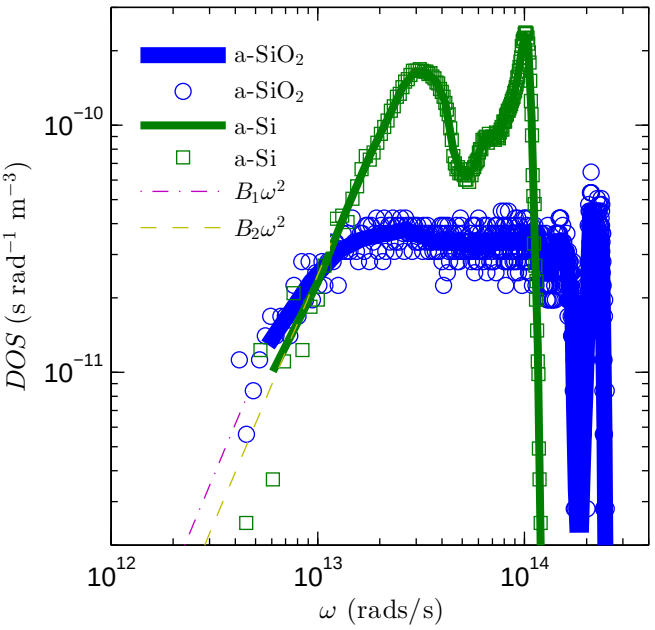

FIG. 1: film thickness dependant thermal conductivity of a-Si from experiment.

compared to transverse modes in a given interval of frequency.(cite)

B. Group Velocity

1. From Elastic Constants and DOS

The transverse and logitudinal sound speeds of a material can be related to the material's elastic constants, which determine the bulk (G) and shear (K) moduli.(cite) The transverse sound speed is given by

$$v_{s,T} = \frac{G}{\rho}^{1/2}, \tag{12}$$

and the longitudinal by

$$v_{s,L} = \frac{4G + 3K}{3\rho}^{1/2}. \tag{13}$$

We use the bulk and shear moduli defined in terms of the elastic constants according to the Voight convention.(cite) The sound speeds calculated from the elastic constants are reported in Table . It is clear that the DOS of our models for a-Si and a-SiO_2 are characterized by using the transverse sound speeds, rather than an averaging of the two,

$$v_s = \frac{1}{3}v_{s,L} + \frac{1}{3}v_{s,T}. \tag{14}$$

This is backed up by theoretical(cite) and experimental(cite) results.

2. From Struture Factor

For a disordered solid, the three acoustic group velocities (two transverse and one longitudinal) can be predicted using the elastic constants[?] or by finite differencing of the three lowest frequency branches of the dispersion relation of the supercell.[14?] Except for this low-frequency behavior, there is not an accepted method to predict the group velocity of a vibrational mode in a disordered system, although there have been attempts.[14? ? ? ,15] In the Cahill-Pohl (CP) model, for example, the group velocity of all disordered modes is the sound speed, v_s, which is also assumed for the HS model, Eq. (9).[15] This assumption is not generally valid for any material.[13? ? ? ,14]

Calculating the structure factors of the supercell Gamma modes is a method to test for their plane-wave character at a particular wave vector and polarization corresponding to the VC.[13,19] Feldman et al. used the structure factor to predict an effective dispersion for a model of amorphous silicon, but did not predict group velocities.[13] Volz and Chen used the dynamic structure factor to predict the dispersion of crystalline SW silicon using MD simulation.[?]

The structure factor at a VC wave vector $\boldsymbol{\kappa}_{VC}$ is defined as[19]

$$S^{L,T} = \sum_{\nu} E^{L,T}\delta[\omega - \omega], \tag{15}$$

where the summation is over the Gamma modes, E^T refers to the transverse polarization and is defined as

$$E^L = \left| \sum_b \hat{\boldsymbol{\kappa}}_{VC} \cdot e \exp\left[i\boldsymbol{\kappa}_{VC} \cdot \boldsymbol{r}_0\left(\begin{smallmatrix} l=0 \\ b \end{smallmatrix}\right)\right] \right|^2 \tag{16}$$

and E^L refers to the longitudinal polarization and is defined as

$$E^T = \left| \sum_b \hat{\boldsymbol{\kappa}}_{VC} \times e \exp\left[i\boldsymbol{\kappa}_{VC} \cdot \boldsymbol{r}_0\left(\begin{smallmatrix} l=0 \\ b \end{smallmatrix}\right)\right] \right|^2. \tag{17}$$

In Eqs. (16) and (17), the b summations are over the atoms in the disordered supercell, $\boldsymbol{r}_0\left(\begin{smallmatrix} l=0 \\ b \end{smallmatrix}\right)$ refers to the equilibrium atomic position of atom b in the supercell, l labels the unit cells ($l = 0$ for the supercell), α labels the Cartesian coordinates, and $\hat{\boldsymbol{\kappa}}_{VC}$ is a unit vector. Explicit disorder is included in the Gamma frequencies ω and the $3N_a$ components of the eigenvectors, e.

Fig 4 of this work shows a dispersion extracted by locating the peaks in the structure factor.[17]

Fig. 5 discusses how since the low freq modes are sparse, there is a resonant effect between[13]

The structure factor gives the frequency spectrum needed to construct a (nonstationary) propagating state with a pure wave vector Q and pure longitudinal or transverse polarization[12]. Locations of spectral peaks are

TABLE I: Estimated from the elastic constants, the pre-annealed group velocities are $v_{s,T,} = 3,670$, $v_{s,L,elas} = 7,840$ $v_{s,T,elas} = 2,541$, $v_{s,L,elas} = 4,761$ (see Section).

method	B_{mod} (Eq. (??))	$S_{T,L}$ (Eq. (15), (19))	DOS (Eq. (11))
a-SiO_2			
transverse	3,161	2,732	2,339
longitudinal	5,100	4,779	
a-Si			
transverse	3,886	3,699	3,615
longitudinal	8,271	8,047	

peaked like a acoustic dispersion branches. Only low-frequency vibrations have an (approximate) wavevector in disordered systems, and there is no theorem guranteeing this.[13]

However, it is very difficult to distinguish between localized and extended modes at high frequencies on the basis of their $S(k,\nu)$ functions, as illustrated by the very similar scattering functions for a 67-meV localized and a 63-meV extended mode in Fig. 3(b).[18]

The dynamic structure factor can be useful for demonstrating the plane-wave character of low-frequency vibrations. However, on a mode-by-mode basis, it is unable in general to characterize a given mode as either localized or delocalized. Thus, it is not possible to

$$\mathbf{v}_{g,\mathbf{n}}(\boldsymbol{\kappa}_\nu) = \frac{\partial\omega(\boldsymbol{\kappa}_\nu)}{\partial\boldsymbol{\kappa}}. \tag{18}$$

estimates of the sound speeds are found from using finite difference of the peaks in $S_{T,L}$ for different values of k.

A group velocity can be assigned by taking a slope of a graph of peak frequency versus wave vector.[12]

$$\mathbf{v}_{g,\mathbf{n}}(\boldsymbol{\kappa}_\nu) = \frac{\partial\omega(\boldsymbol{\kappa}_\nu)}{\partial\boldsymbol{\kappa}}. \tag{19}$$

Table **??**.

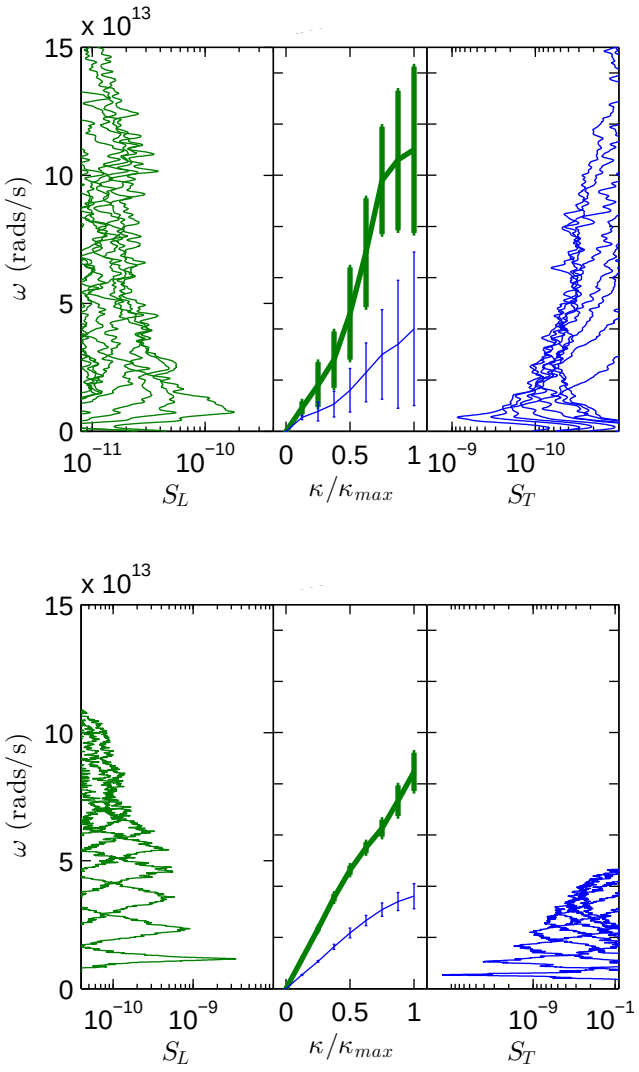

FIG. 2: film thickness dependant thermal conductivity of a-Si from experiment.

C. Mode Lifetimes

1. *From Structure Factor*

beltukov which is a constant related to the DOS.**?**

2. *From Normal Mode Decomposition*

We use the MD simulation-based NMD method to predict the lifetimes .[20–23] In NMD, the atomic trajectories are first mapped onto the vibrational mode coordinate time derivative,[24]

$$\dot{q}(\boldsymbol{\kappa}_\nu;t) = \sum_{\alpha,b,l}^{3,n,N} \sqrt{\frac{m_b}{N}}\dot{u}_\alpha(\begin{smallmatrix}l\\b\end{smallmatrix};t)\, e^*(\begin{smallmatrix}\boldsymbol{\kappa} & b\\ \nu & \alpha\end{smallmatrix}) \exp[i\boldsymbol{\kappa}\cdot\mathbf{r}_0(\begin{smallmatrix}l\\0\end{smallmatrix})]. \tag{20}$$

Here, m_b is the mass of the b_{th} atom in the unit cell, u_α is the α-component of the atomic displacement from equilibrium, $\dot{u}_\alpha$ is the α-component of the atomic velocity, and t is time.

The spectral energy of each vibrational mode, $\Phi(\boldsymbol{\kappa}_\nu;t)$, is calculated from

$$\Phi(\boldsymbol{\kappa},\omega) = 2\sum_{\nu}^{3n} T(\boldsymbol{\kappa}_\nu;\omega) = 2\sum_{\nu}^{3n}\lim_{\tau_0\to\infty}\frac{1}{2\tau_0}\left|\frac{1}{\sqrt{2\pi}}\int_0^{\tau_0}\dot{q}(\boldsymbol{\kappa}_\nu;t)\exp(-i\omega t)\right. \tag{21}$$

The vibrational mode lifetime is predicted by fitting each mode's spectral energy $\Phi(\nu,\omega)$ to a Lorentzian function

$$\Phi(\nu,\omega) = \sum_{\nu}^{3n}\frac{C_0(\nu)}{[\omega_0(\nu)-\omega]^2+\Gamma^2(\nu)}, \tag{22}$$

where the constant $C_0(\nu)$ is related to the average energy of each mode and the linewidth $\Gamma(\nu)$.[23] The mode lifetime is given by

$$\tau(\nu) = \frac{1}{2\Gamma(\nu)} \tag{23}$$

Lifetimes in amorphous silicon predicted before using a normal mode approach, but mode-by-mode properties were not presented.[25]

Lifetimes were predicted using anharmonic lattice dynamics, but no thermal transport properties were predicted.[26]

The lifetimes of vibrational modes in a-Si were predicted using normal mode decomposition.[14]

"The modes of mixed character which lie outside or in between the central groups of pure plane-wave modes are typically resonances as indicated by the large values of 1/p i . How- ever, these modes are also reasonably well interpreted as filling in the appropriate tails of Lorentzian response func- tions, modulo small statistical fluctuations to be expected in finite systems. bigger and small Q s become less sparse, Lorentzians of fixed width will overlap increasingly, and can force out the resonant states which otherwise would inhabit the gaps. For Q of order 1/L there will always be gaps, no matter how big the system L see for instance the region near 4.1 meV in Fig. 6 where a resonance occurs, but these gaps drift toward Q 0 and 0 as L increases. Therefore the distinction between special frequencies lying in gaps, and other frequen- cies lying in Lorentzian peaks, must disappear as L increases. There are two possibilities: either resonant behavior entirely disappears, or else it remains in a diluted form and is shared uniformly by all the normal modes. That is, at any given frequency there may be isolated parts of a large sample which are particularly sensitive to oscillation at just this fre- quency and temporarily trap selected traveling waves of this frequency. If this behavior is found for all normal modes, then any one normal mode will be freely propagating almost everywhere, and it becomes a subtle matter of definition or taste whether they should be called resonances at all. "s

"To implement Eq. 6 one must know the correct Q dependence of Q . As shown in Fig. 8, the fitted values scatter too much to guide the extrapolation well. In principle, at very small Q one should get a form Q CQ 4 which corresponds to Rayleigh scattering of sound waves from the structural disorder. The data of Fig. 8 do not fit a Q 4 law; the Q 2 curve shown in the figure is a better fit. Two experiments13,15 but not a third35 and one calculation18 on a-SiO2 have also given Q 2 . We do not know a theory which can give this law in a harmonic model.

"The conclusion is that intrinsic harmonic glassy disorder contained in our finite calculation kills off the heat-carrying ability of propagons rapidly enough without invoking any exotic mechanism. Our (T) curve is reminiscent of the ex- periments of Zaitlin and Anderson after holes are introduced to enhance the elastic damping of long-wavelength modes. The plateau disappears from their data in much the same way that it disappears from our theory due to extra damping of small-Q propagons.

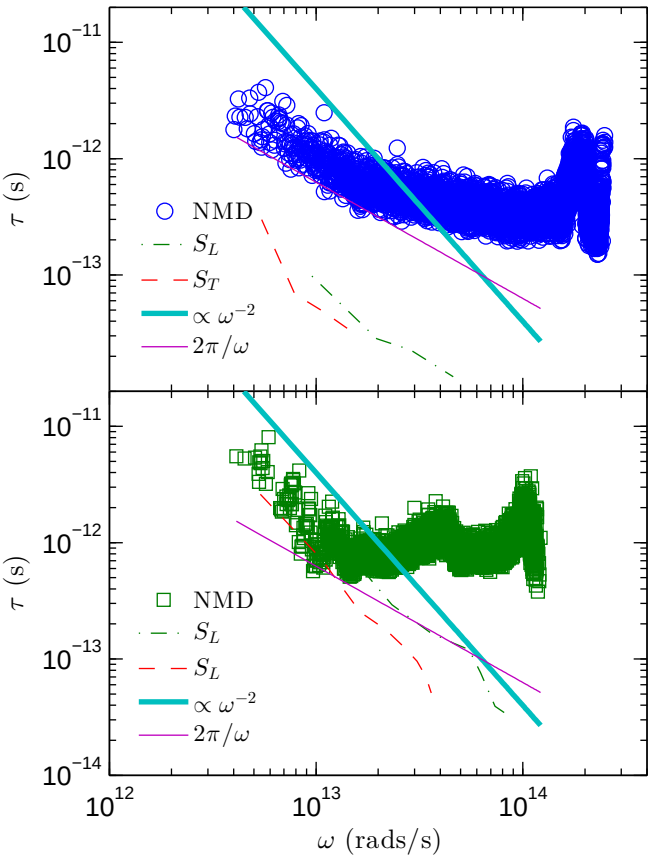

FIG. 3: film thickness dependant thermal conductivity of a-Si from experiment.

D. Diffusivities

Thermal diffusivity was predicted for a percolation network which showed Rayleigh type scattering dependance in the low-frequency limit.[27]

Thermal diffusivity has been predicted using a wave-packet method

E. Mean Free Paths

Using the lifetimes predicted from the structure factor peaks and the transverse sound speed, the MFP is about the size of the simulation cell L.

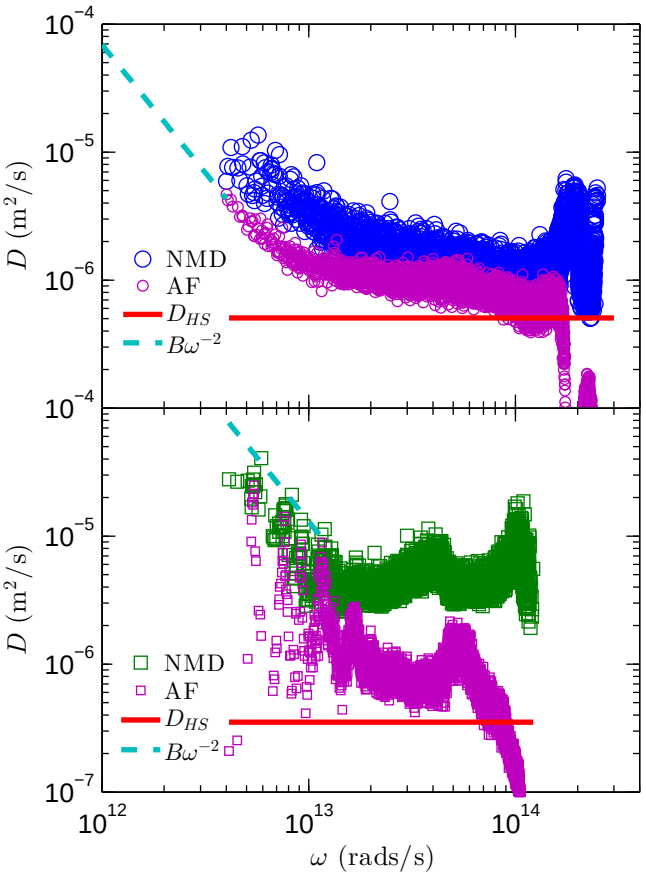

FIG. 4: film thickness dependant thermal conductivity of a-Si from experiment.

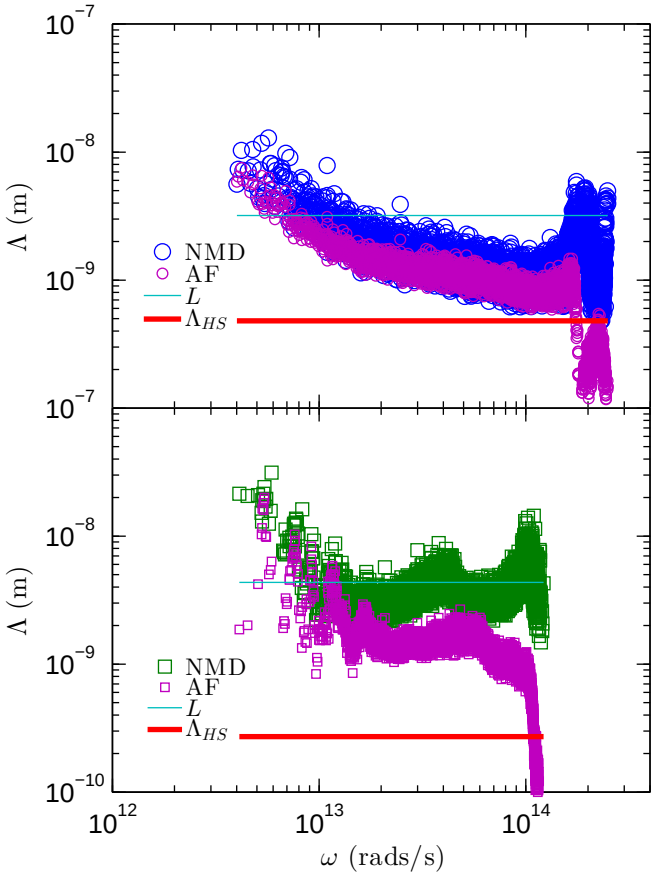

FIG. 5: film thickness dependant thermal conductivity of a-Si from experiment.

V. THERMAL CONDUCTIVITY

A. Bulk

We use the GK method to predict the thermal conductivity. The GK method is relatively inexpensive compared to the NMD and AF methods so that large system sizes can be simulated (see Section).

For smaller system sizes, the same trajectories are used for the GK and NMD methods. The MD simulations were run with the same parameters as the NMD metho (see Section).

The predicted thermal condcutivties from the GK method are plotted in Fig. . For a-SiO2, the thermal conductivity is size independent within the errors. For a-Si, there is a clear size-dependance of the thermal conductivity

To compare the results of the mode-based methods (NMD and AF) and the GK method, it is necessary to estimate the missing contribution from vibrational modes with frequency less than the minimum frequency of the finnite systems.

Assuming the thermal conductivity form Eq. for the lowest frequency modes in the system, the thermal conductivity as a function of the system size takes the form

$$\frac{k(N_0)}{k_{bulk}} = 1 - \frac{c_0}{N_0}, \tag{24}$$

"We find that we cannot define a wave vector for the majority of the states, but the intrinsic harmonic diffusivity is still well-defined and has a numerical value similar to what one gets by using the Boltzmann result, replacing v by a sound velocity and replacing l by an interatomic distance a. "[12]

"In order to fit the experimental sc(T) it is necessary to add a Debye- like continuation from 10 meV down to 0 meV. The harmonic diffusivity becomes a Rayleigh m law and gives a divergent (T) as T O. To eliminate this we make the standard assumption of resonant- plus-relaxational absorption from two-level systems (this is an anharmonic effect which would lie outside our model even if it did contain two-level systems implicitly). "[12]

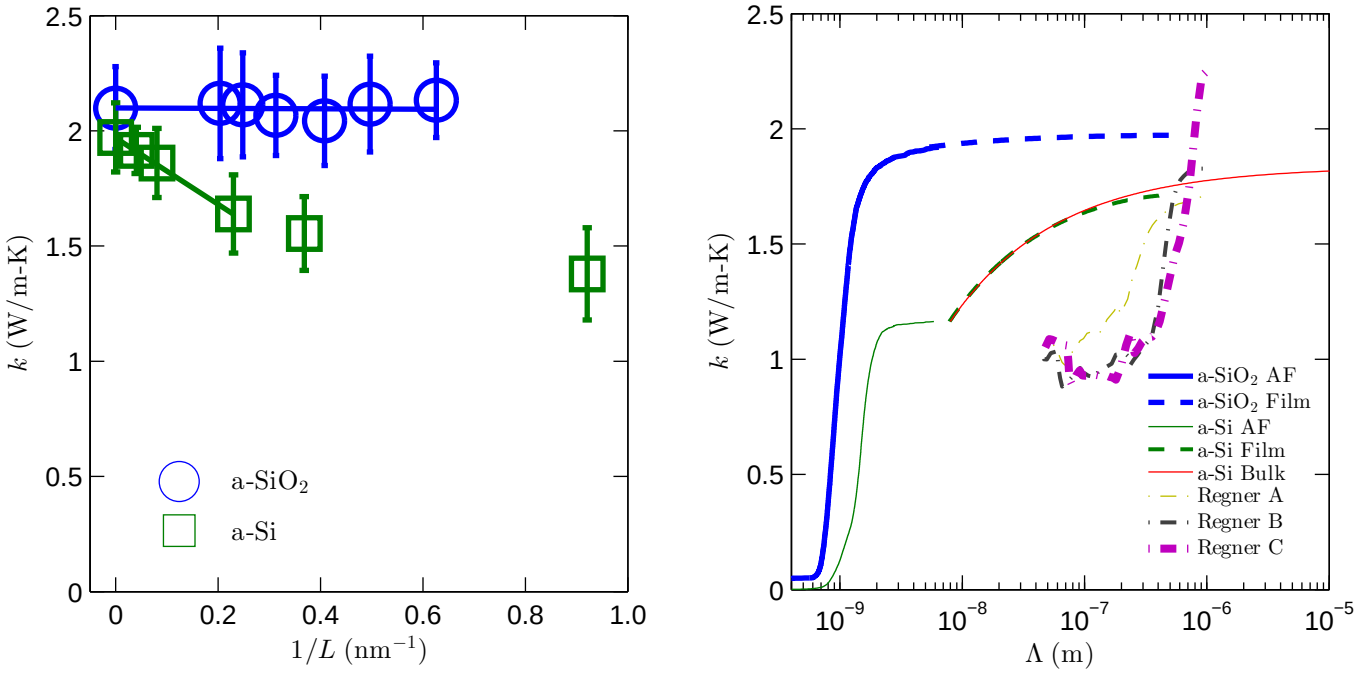

FIG. 7: film thickness dependant thermal conductivity of a-Si from experiment.

$$k = \int_0^{\omega_{cut}} \frac{d\omega DOS(\omega)C(\omega)D(\omega)}{V} + \frac{1}{V}\sum_i C(\omega)D(\omega) \tag{25}$$

Debye model. $k_tot = k_phonon + k_AF. For lack of a rigorous definition of phonon vs diffusion, we will define k_phon = k_debye.$

B. Accumulation

C. Discussion

VI. SUMMARY

Table **??**.

* Electronic address: mcgaughey@cmu.edu

[1] J. J. Freeman and A. C. Anderson, Physical Review B **34**, 5684\textbackslash965690 (1986).

[2] D. G. Cahill, S. K. Watson, and R. O. Pohl, Phys. Rev. B **46**, 61316140 (1992), URL http://link.aps.org/doi/10.1103/PhysRevB.46.6131.

[3] H. Wada and T. Kamijoh, Japanese Journal of Applied Physics **35**, L648L650 (1996), URL http://jjap.jsap.jp/link?JJAP/35/L648/.

[4] B. L. Zink, R. Pietri, and F. Hellman, Physical Review Letters **96**, 055902 (2006), URL http://link.aps.org/doi/10.1103/PhysRevLett.96.055902.

[5] H.-S. Yang, D. G. Cahill, X. Liu, J. L. Feldman, R. S. Crandall, B. A. Sperling, and J. R. Abelson, Phys. Rev. B **81**, 104203 (2010), URL http://link.aps.org/doi/10.1103/PhysRevB.81.104203.

[6] D. G. Cahill, M. Katiyar, and J. R. Abelson, Physical Review B **50**, 60776081 (1994).

[7] B. S. W. Kuo, J. C. M. Li, and A. W. Schmid, Applied Physics A: Materials Science & Processing **55**, 289296 (1992), ISSN 0947-8396, 10.1007/BF00348399, URL http://dx.doi.org/10.1007/BF00348399.

[8] S. Moon, International Journal of Heat and Mass Transfer **45**, 24392447 (2002), URL http://linkinghub.elsevier.com/retrieve/pii/S001793100100347X.

[9] X. Liu, J. L. Feldman, D. G. Cahill, R. S. Crandall, N. Bernstein, D. M. Photiadis, M. J. Mehl, and D. A. Papaconstantopoulos, Phys. Rev. Lett. **102**, 035901 (2009), URL http://link.aps.org/doi/10.1103/PhysRevLett.102.035901.

[10] J. M. Ziman, *Electrons and Phonons* (Oxford, New York, 2001).

[11] P. B. Allen and J. L. Feldman, Physical Review B **48**, 1258112588 (1993).

[12] J. L. Feldman, M. D. Kluge, P. B. Allen, and F. Wooten, Physical Review B **48**, 1258912602 (1993).

[13] J. L. Feldman, P. B. Allen, and S. R. Bickham, Phys. Rev. B **59**, 35513559 (1999), URL http://link.aps.org/doi/10.1103/PhysRevB.59.3551.

[14] Y. He, D. Donadio, and G. Galli, Applied Physics Letters **98**, 144101 (2011).

[15] D. Cahill and R. Pohl, Annual Review of Physical Chemistry **39**, 93121 (1988).

[16] S. Plimpton, Journal of Computational Physics **117**, 1 19 (1995), ISSN 0021-9991, URL http://www.sciencedirect.com/science/article/pii/S002199918

[17] V. Vitelli, N. Xu, M. Wyart, A. J. Liu, and S. R. Nagel, Phys. Rev. E **81**, 021301 (2010), URL http://link.aps.org/doi/10.1103/PhysRevE.81.021301.

[18] R. Biswas, A. M. Bouchard, W. A. Kamitakahara, G. S. Grest, and C. M. Soukoulis, Phys. Rev. Lett. **60**, 22802283 (1988), URL http://link.aps.org/doi/10.1103/PhysRevLett.60.2280.

[19] P. B. Allen, J. L. Feldman, J. Fabian, and F. Wooten, Philosophical Magazine B **79**, 17151731 (1999).

[20] A. J. C. Ladd, B. Moran, and W. G. Hoover, Physical Review B **34**, 50585064 (1986).

[21] A. J. H. McGaughey and M. Kaviany, Physical Review B **69**, 094303 (2004).

[22] J. E. Turney, PhD thesis, Carnegie Mellon University, Pittsburgh, PA (2009).

[23] J. M. Larkin, J. E. Turney, A. D. Massicotte, C. H. Amon, and A. J. H. McGaughey, to appear in Journal of Computational and Theoretical Nanoscience (2012).

[24] M. T. Dove, *Introduction to Lattice Dynamics* (Cambridge, Cambridge, 1993).

[25] S. R. Bickham and J. L. Feldman, Phys. Rev. B **57**, 1223412238 (1998), URL http://link.aps.org/doi/10.1103/PhysRevB.57.12234.

[26] J. Fabian and P. B. Allen, Phys. Rev. Lett. **77**, 38393842 (1996), URL http://link.aps.org/doi/10.1103/PhysRevLett.77.3839.

[27] P. Sheng and M. Zhou, Science **253**, 539542 (1991), URL http://www.sciencemag.org/content/253/5019/539.abstract.